

## Structural evaluation of Aspendos (Belkıs) Masonry Bridge

Temel Türker\*

*Department of Civil Engineering, Karadeniz Technical University, 61080, Trabzon, Turkey*

*(Received June 23, 2013, Revised March 23, 2014, Accepted March 26, 2014)*

**Abstract.** In this study, the structural performance of a seven span masonry arch bridge was evaluated. Investigations were performed on Aspendos (Belkıs) Masonry Arch Bridge which was located on road of Aspendos Acropolis City in Antalya, Turkey. The old bridge was constructed in the early of fourth century AD, but it was exposed to the earthquakes in this region and the overloading by the river water. The old bridge was severely damaged and collapsed by probably an earthquake many years ago and a new bridge was then reconstructed on the remains of this old bridge by Seljuk in the 13th century. The bridge has also been affected from overflowing especially in the spring of each year, so some protective measures should be taken for this monumental bridge. Therefore, the structural performance under these loading has to be known. For this purpose, an initial finite element model was developed for the bridge and it was calibrated according to ambient vibration test results. After that, it was analyzed for different load cases such as dead, live, earthquake and overflow. Three load combinations were taken into account by deriving from these load cases. The displacements and the stresses for these combination cases were attained and compared with each other. The structural performance of Aspendos Masonry Arch Bridge was determined by considering the demand-capacity ratio for the tensile stress of the mortar used in Aspendos Masonry Arch Bridge. After these investigations, some concluding remarks and offers were presented at the end of this study.

**Keywords:** finite element modeling; masonry bridges; model calibration; structural performance; tensile stress

---

### 1. Introduction

Anatolia is a paradise of historical structures. There are many mosques, churches and arch bridges, made of masonry stones, from Seljuk, Roma, and Ottoman. These historical structures particularly susceptible to the damages induced from aging and environmental effects such as earthquake, over flow, over loading. These loads may yield partial or total collapse of these structures. To protect the structures, the repairing and/or restoration applications have to be applied to the historical structures. But, the application projects usually aim to regain the original appearance rather than improve the static and dynamic behavior of these structures. Therefore, the projects should be evaluated in view of the static and dynamic behavior.

Masonry bridges are generally able to carry the vertical loads in a very safe and stable way because of high compressive strength of stone while they are rather sensitive to lateral loads. Therefore, they were used traditionally to pass long span in arch structural form. The most known

---

\*Corresponding author, Assistant Professor, E-mail: [temelturker@ktu.edu.tr](mailto:temelturker@ktu.edu.tr)

arch type masonry bridges in Turkey are Çifte Bridge in Artvin, Mikron Bridge in Rize, Koyunbaba Bridge in Çorum, Kemere Bridge in Bartın, Justinianus Bridge in Sakarya, Büyükçekmece Bridge in İstanbul, Sultan Süleyman Bridge in İstanbul, Uzun Bridge in Edirne, Belkıs Bridge in Antalya, Kesik Bridge in Sivas, Ceyhan Bridge in Kahramanmaraş, Malabadi Bridge in Diyarbakır (URL-1). A good example of the arch bridge of Ottoman time in Europe is Mostar Bridge in Bosnia-Herzegovina (URL-2). Most of the masonry arch bridge was constructed in long stream beds and supported by many times. Therefore, water pressure in the lateral direction creates unsatisfied loading condition for these structures. Especially, the river water in big rivers generates high level lateral loads on the masonry bridges, which may cause the overturn. Similarly, the scouring on supports creates unsuitable cases for the bridges (Alberto *et al.* 2010). Also, the masonry arch bridges were severely affected from earthquake because of the high amount mass of the structural members (Rota 2004, Pela *et al.* 2009). These effects may cause outer and/or inner cracks on the structural system of the masonry bridges.

It is known that the structural behavior is identified by using the mechanical and geometrical properties of these structures. Finite element modeling and analyzing is the one of the most effective method. But simplified assumptions for the boundary conditions, material properties and connections in structural members cause inaccurate structural identification and the restoration applications cannot reach the goal. So, the initial finite element models need calibration according to the exact structural parameters to reflect the real structural behavior. In many studies in literature on the masonry structures, it was addressed that the results from the calibrated finite element models are in the harmony and represent the real behavior of structure more accurately. Ramos *et al.* (2005) studied damage detection of a masonry construction by using operational modal analysis. The masonry model was built with limestone units. Finite-element analysis and modal testing were carried out to extract the analytical and experimental dynamic characteristics. Tanaro Masonry Bridge built in 1866 was investigated both in service conditions and at different stages of its demolition (Brencich and Sabia 2008). The natural frequencies, mode shapes, and damping ratios were identified by dynamic tests. The analytical modeling, modal testing, and finite-element model updating of masonry arch bridges were presented by Bayraktar *et al.* (2009). Finite-element model of the bridges were updated to minimize the differences between analytically and experimentally estimated dynamic characteristics by changing boundary conditions.

To calibrate finite element models, generally the dynamic characteristics, such as natural frequencies, mode shapes, and modal damping ratios, were preferred to use. The dynamic parameters were determined by ambient vibration test under environmental loads, such as wind, traffic and any damaged effects cannot be created on the investigated structures (Bayraktar *et al.* 2010). Structural performance of masonry structures can be determined by analyzing the most vulnerable parameter, such as tensile stress, displacement, etc., for different cases and checking the maximum values after calibrating the finite element model. For the masonry arch bridges, the parameter could be selected as tensile stress of the mortar because of the low tensile strength (Rota 2005, Pela *et al.* 2012).

The study aims to present the structural performance of Aspendos (Belkıs) Masonry Arch Bridge. The bridge was exposed to earthquakes in the region and overloading by the river water especially in the spring of each year. Also, it was observed the scouring on supports. It may be occurred some cracks on the bridge. A finite element model of the bridge was developed and calibrated according to the ambient vibration test results. The model was analyzed for dead, live, earthquake and overflow load cases. The structural performance was evaluated by considering the maximum tensile stresses of the mortar.

## 2. Formulation of modal parameter identification

Several modal parameter identification techniques are available for extracting dynamic characteristics from ambient vibration data. In this study, Enhanced Frequency Domain Decomposition (EFDD) in the frequency domain are used to extract the dynamic characteristics of the bridge. Enhanced Frequency Domain Decomposition technique is an extension to Frequency Domain Decomposition (FDD) technique, which is a basic technique that is extremely easy to use. In the technique, modes are simply picked locating the peaks in Singular Value Decomposition plots (SVD) calculated from the spectral density spectra of the responses. As FDD technique is based on using a single frequency line from the Fast Fourier Transform analysis (FFT), the accuracy of the estimated natural frequency depends on the FFT resolution and no modal damping is calculated. However, EFDD technique gives an improved estimation of both the natural frequencies, the mode shapes and includes the damping ratios (Peeters 2000, Jacobsen *et al.* 2006).

In EFDD technique, the single degree of freedom (SDOF) Power Spectral Density (PSD) function, identified around a peak of resonance, is taken back to the time domain using the Inverse Discrete Fourier Transform (IDFT). The natural frequency is obtained by determining the number of zero-crossing as a function of time, and the damping by the logarithmic decrement of the corresponding SDOF normalized auto correlation function (Jacobsen *et al.* 2006). In EFDD technique, the relationship between the unknown input and the measured responses can be expressed as

$$G_{yy}(j\omega) = H(j\omega)^* G_{xx}(j\omega)H(j\omega)^T \quad (1)$$

where  $G_{xx}(j\omega)$  is the Power Spectral Density (PSD) matrix of the input,  $G_{yy}(j\omega)$  is the PSD matrix of the responses,  $H(j\omega)$  is the Frequency Response Function (FRF) matrix, \* and superscript  $T$  denote complex conjugate and transpose, respectively. The FRF can be written in partial fraction, i.e., pole/residue form

$$H(j\omega) = \sum_{k=1}^n \frac{R_k}{j\omega - \lambda_k} + \frac{R_k^*}{j\omega - \lambda_k^*} \quad (2)$$

where  $n$  is the number of modes  $\lambda_k$  is the pole,  $R_k$  is the residue. Then Eq. (1) becomes as

$$G_{yy}(j\omega) = \sum_{k=1}^n \sum_{s=1}^n \left[ \frac{R_k}{j\omega - \lambda_k} + \frac{R_k^*}{j\omega - \lambda_k^*} \right] G_{xx}(j\omega) \left[ \frac{R_s}{j\omega - \lambda_s} + \frac{R_s^*}{j\omega - \lambda_s^*} \right]^{\bar{H}} \quad (3)$$

where  $s$  is the singular values, superscript  $H$  denotes complex conjugate and transpose. Multiplying the two partial fraction factors and making use of the Heaviside partial fraction theorem, after some mathematical manipulations, the output PSD can be reduced to a pole/residue form as follows

$$G_{yy}(j\omega) = \sum_{k=1}^n \frac{A_k}{j\omega - \lambda_k} + \frac{A_k^*}{j\omega - \lambda_k^*} + \frac{B_k}{-j\omega - \lambda_k} + \frac{B_k^*}{-j\omega - \lambda_k^*} \quad (4)$$

where  $A_k$  is the  $k$  th residue matrix of the output PSD. In the EFDD identification, the first step is to estimate the PSD matrix. The estimation of the output PSD known at discrete frequencies is



Fig. 1 The ruins of the old Aspendos Bridge

then decomposed by taking the SVD of the matrix

$$G_{yy}(j\omega_i) = U_i S_i U_i^H \quad (5)$$

where the matrix  $U_i = [u_{i1}, u_{i2}, \dots, u_{im}]$  is a unitary matrix holding the singular vectors  $u_{ij}$ , and  $s_{ij}$  is a diagonal matrix holding the scalar singular values. The first singular vector  $u_{ij}$  is an estimation of the mode shape. PSD function is identified around the peak by comparing the mode shape estimation  $u_{ij}$  with the singular vectors for the frequency lines around the peak. From the piece of the SDOF density function obtained around the peak of the PSD, the natural frequency and the damping can be obtained.

### 3. Aspendos (Belkıs) Masonry Arch Bridge

The Aspendos Masonry Bridge was a late Roman bridge over the Köprüçay River in southern Anatolia. The bridge was situated on the road of Antalya-Manavgat and approximately 2km from Aspendos Acropolis City. It was known as Eurymedon in ancient times. It was damaged and many of its arches collapsed. The bridge lost a lot of former splendor. The shape and course of the old bridge had been reconstructed digitally, based on the still extant remains of the ancient structure: parts of the ramps, the abutments, as well as the foundation of a pier by Kesenner and Piras (1998) and Klaus (1999). Several pieces of the original bridge were found scattered in the river bed. It can be seen some parts of the old bridge in two sides in Fig. 1.

The old bridge had nine semi circular arches and it had a length of 259.50m and a width of 9.44m. It crossed the river in a straight way. The overall height of the old bridge was 4.1m higher than the later Seljuk structure as stated by Klaus (1999). The middle section stood on six arches, complemented on the two sides by three smaller arches, which served as spillways in case the river overflowed. In the normal level of water, the river flowed between the three central arches, constrained by double-wedge-shaped reinforcements of masonry, placed at the two outer pillars and intended to prevent their undermining by the river. These masonry structures were markedly



Fig. 2 Some views from the upstream and downstream faces of Aspendos Bridge

higher on the upstream side (8.15m) than on the downstream (4.76m). In addition, wedge-shaped breakwaters were added on the piers, although not all piers feature them on both sides. The clear spans of the three central arches had been determined at 23.52m for the central arch and 14.95m for the two flanking arches, while the two piers supporting the central arch were measured at 9.60m (URL-3). The old bridge was severely damaged and collapsed probably by an earthquake many years ago.

In the 13th century, a new bridge was constructed by the Seljuk Emperor Alaaddin Keykubat on the foundations and several remnants of the old bridge. The Seljuk builders followed closely the course of the Roman remains, even in sections where the piers had been partly moved downstream from their original position. As a result, the bridge features a quite sharp displacement. This zigzag course, formed by two successive, 90 degree bends, in combination with the pointed arches give the Seljuk-Era Bridge an appearance that is quite distinct from that of its Roman precursor as given in Fig. 2. The new bridge is also considerably reduced in dimensions, something that allowed the full use of the Roman remains. Thus, the reduction of the width to almost half the original made the integration of halfway surviving ancient piers. The medieval arches were also 4.1m lower than the Roman ones, and the length of the bridge was shortened, so that the new bridge ramp began at the place where the Roman structure had already reached its final height level (URL-3).

The bridge was mainly constructed of stone blocks, while parts of the old bridge have been reused including the duct stones, which were built into the new ramp. In the late 1990s, restoration works in the bridge's crumbling breastwork also revealed stone inscriptions in Greek and Arabic. The total length of the bridge is 220m and the width of the bridge varies between 3.5m and 6.5m. It has seven arch spans and the length of the biggest span is approximately 16.5m. Stream water flows from five of these spans and the two spans in the right side is above the stream water level as shown in Figs. 3-4. The biggest span is the second span and it has approximately 16m arch length. The smallest span is the sixth span and it has 5.4m arch length as demonstrated in Fig. 5.



Fig. 3 Stream water flow in five spans



Fig. 4 Views from the spans above the stream water level

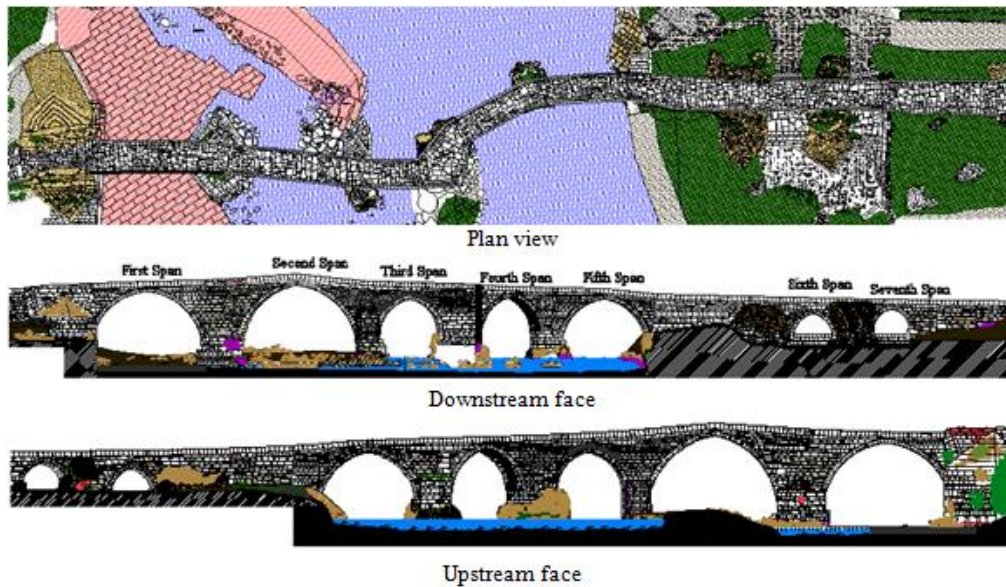


Fig. 5 The detailed drawing of Aspendos Masonry Arch Bridge including water level

The bridge is the most important historical monument in this area and many tourist have visited the bridge every day. It was restored many times in different era. The last two restorations were performed 1998 and 2004. The bridge was damaged by the overflow in 2010. A recent restoration application was performed in the summer of 2011 because of some distortions on the structural system. These distortions create unsuitable case for the important historical masonry bridge.

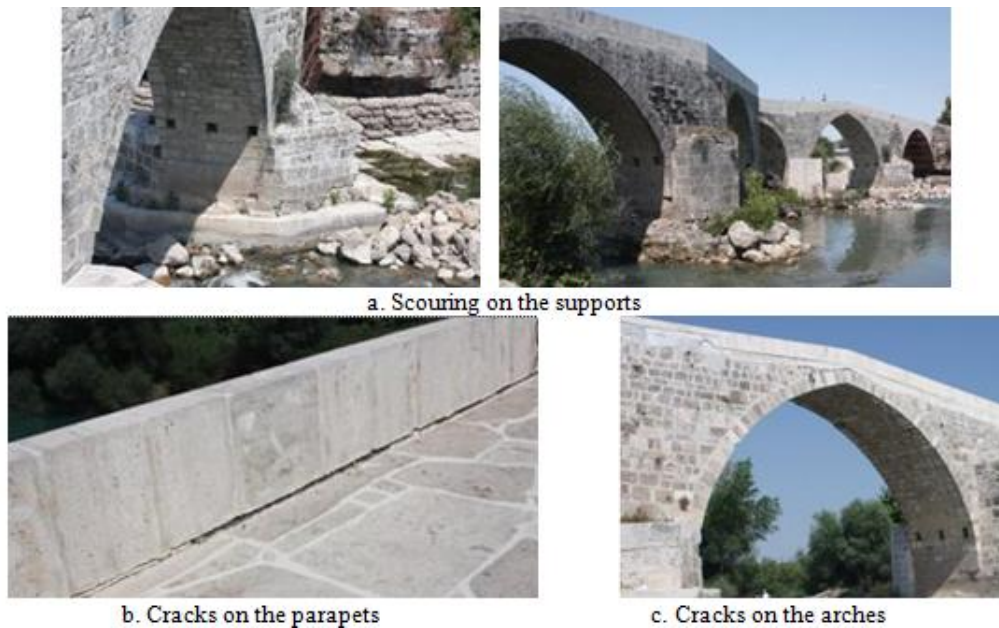


Fig. 6 The damages on Aspendos Masonry Arch Bridge

### 3.1 Distortions on Aspendos Masonry Arch Bridge

There are many distortions on both structural and non-structural members of the bridge. In the flood in 2003, the bridge severely damaged. A restoration application was applied to the bridge. But it was damaged again in the flood in 2010. The current damages occurred after the last flood. Some of them are visual distortions and low level while the others are severe in view of structural behavior. The distortions, such as scouring on the supports, cracks on parapets, arches and walls, joint segregation, mainly come into exist due to stream water pressure. Fig. 6 shows some of the damage on Aspendos Masonry Arch Bridge.

The scouring on the supports caused vertical movements on some parts of the main body and the damages on the arches and walls. The damages concentrated on the second and third spans. It can be clearly seen the disintegration between the parapets and the bridge deck as shown in Figure 6b.

### 3.2 Material properties of the bridge

The bridge consists of many architectural members, such as walls, decks, ledges, parapets, and flood splitter, etc, as given in Fig. 7. The bridge has different type arches constructed according to Roma and Seljuk times. Also, there are different types of stones on main body of the bridge because of the restoration applications in different times.

In the laboratory investigations, it was determined that the maximum compressive stress of the masonry stones and the mortars were 46MPa and 4.1MPa, respectively. Also, it was assumed that the maximum tensile stress of the mortars was 0.41MPa. The mechanical properties, such as elasticity modulus, Poisson ratio and mass density, of the bridge were determined as given in Table 1.



Fig. 7 The architectural members in Aspandos Masonry Arch Bridge

Table 1 The material properties of Aspandos Masonry Arch Bridge

Members	Elasticity Modulus (N/m <sup>2</sup> )	Poisson Ratios	Mass Density (kg/m <sup>3</sup> )
Foundations	$8.0 \cdot 10^9$	0.25	1800
Arches	$1.5 \cdot 10^{10}$	0.20	1900
Walls	$1.5 \cdot 10^{10}$	0.20	1900
Cornices	$2.2 \cdot 10^{10}$	0.20	2300
Parapets	$2.2 \cdot 10^{10}$	0.20	2300
Filler	$6.0 \cdot 10^9$	0.15	1600

### 3.3 Loading cases on Aspandos Masonry Arch Bridge

The bridge was exposed to the dead load, live load from human activity especially tourism activity, earthquake load occurred in this region and the overloading by the river water especially

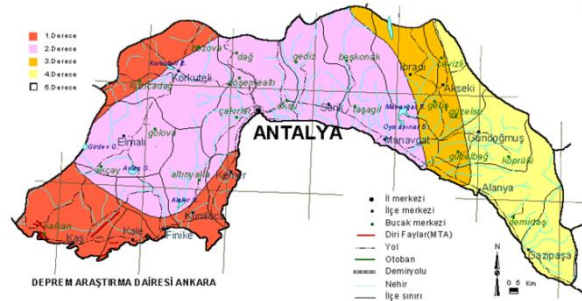


Fig. 8 The definition of the earthquake region of Antalya



Fig. 9 Views from the river water and permanent fortifications in river bed

in the spring of each year. The bridge was located in Antalya, which is in the second earthquake region defined by Turkish Earthquake Guide (DBYBHY 2007), as given in Fig. 8.

### 3.4 Information about river flow and river bed

The bridge has seven spans and only five of those are in use in normal time. In this portion of the river, the speed of flow is very high. To decrease flowing speed, the permanent fortifications were constituted as shown in Fig. 9. The maximum water level in the Köprüçay River was 6.4m.

Information about the river bed was attained from a drilling report for neighboring area. It can be said that the river bed consists of silt, sand and natural coarse aggregate.

## 4. Finite element modeling and analyses

A finite element model of Aspendos Masonry Arch Bridge was developed by using the dimensions on the building surveys and a detailed model was created by SAP2000 Finite Element Program as shown in Fig. 10 (SAP2000 2008). The finite element model consists of four nodes solid elements having three degree of freedom in each node. In the finite element model, totally 9098 finite elements were used. The finite element model was named as initial finite element model because of the many assumptions in boundary conditions, material properties, etc.

Firstly, the initial finite element was analyzed to determine the natural frequencies and mode shapes. Table 2 presents the initial analytical natural frequencies of Aspendos Masonry Arch Bridge.

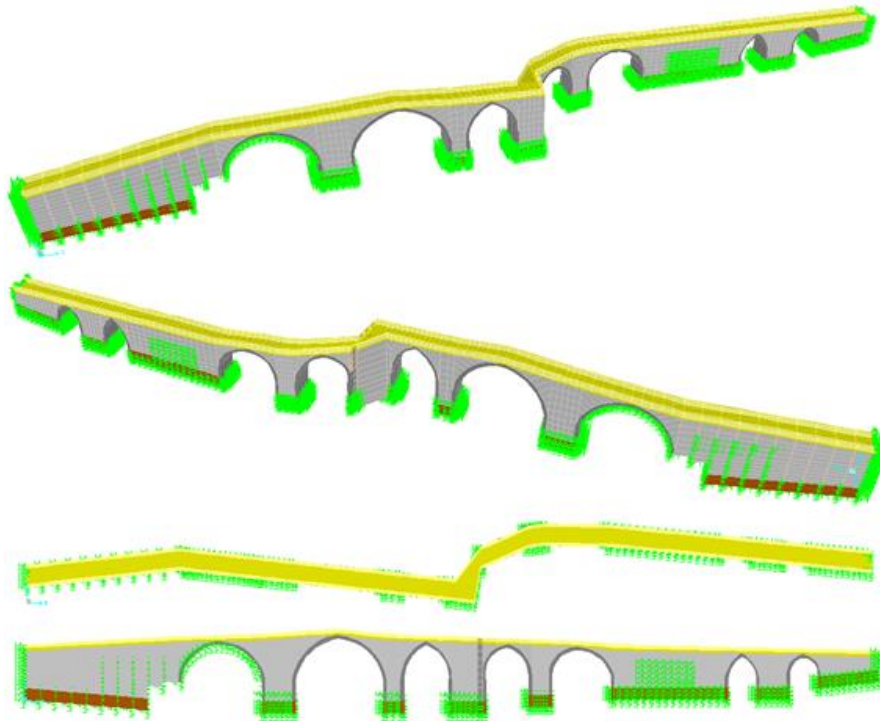


Fig. 10 The finite element model of Aspendos Masonry Arch Bridge

Table 2 The initial analytical natural frequencies of Aspendos Masonry Arch Bridge

Mode Number	Natural Frequency (Hz)
1	9.12
2	15.03
3	16.58
4	17.04
5	21.91

These results in Table 2 were compared with the ambient vibration test results. The test was carried out during the in-situ investigations on the damaged bridge to identify the real dynamic characteristics. The structural responses were acquired by using uniaxial seismic accelerometers from the thirteen different points in vertical and lateral directions. A simplified model for the accelerometer positions on Aspendos Masonry Arch Bridge are given in Fig. 11. Also, some views from the measurement are presented in Fig. 12.

The collected signals were analyzed by using PULSE and OMA software (PULSE 2006; OMA 2006). The natural frequencies, mode shapes and modal damping ratios of the bridge were attained from the signals by Enhanced Frequency Domain Decomposition method in 0-12.5Hz frequency range. The singular values of spectral density matrices are plotted in Fig. 13 for the test. The investigations were reported by Bayraktar (2011). The natural frequencies and the modal damping ratios of the bridge were given in Table 3. Also, the first five mode shapes of the bridge were presented in Fig. 14.

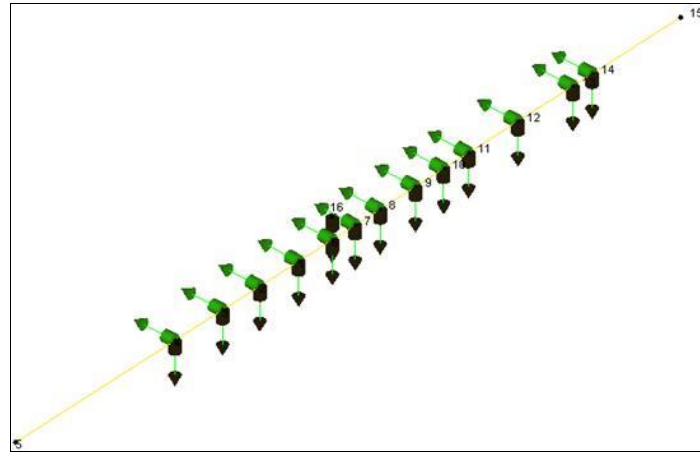


Fig. 11 The accelerometer positions in the measurement of Aspendos Masonry Arch Bridge



Fig. 12 The accelerometer connections on Aspendos Masonry Arch Bridge

[dB | (1 m/s<sup>2</sup>)<sup>2</sup> / Hz]Enhanced Frequency Domain Decomposition - Peak Picking  
Singular Values of Spectral Density Matrices  
of Data Set: Measurement 2

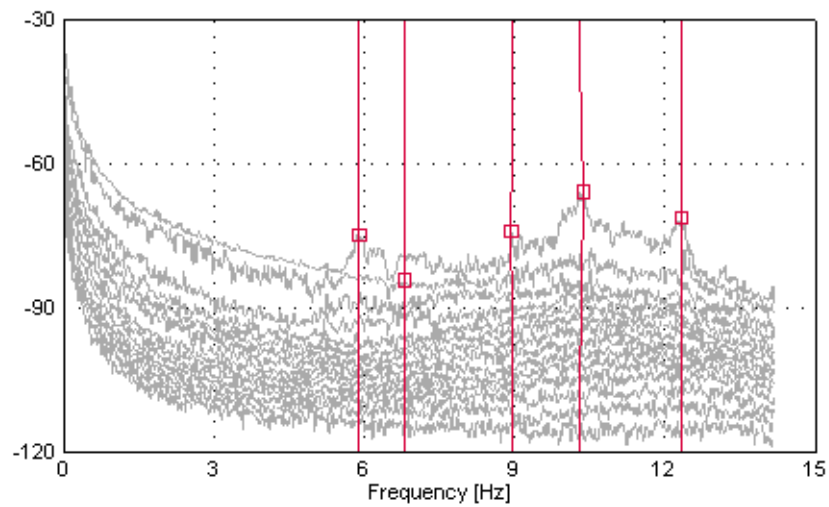


Fig. 13 The singular values of spectral density matrices of Aspendos Masonry Arch Bridge

Table 3 The experimental natural frequencies and modal damping of Aspendos Masonry Arch Bridge

Mode Numbers	Natural Frequency (Hz)	Modal Damping Ratio (%)
1	5.89	1.78
2	6.81	0.20
3	8.94	0.15
4	10.28	2.24
5	12.32	0.27

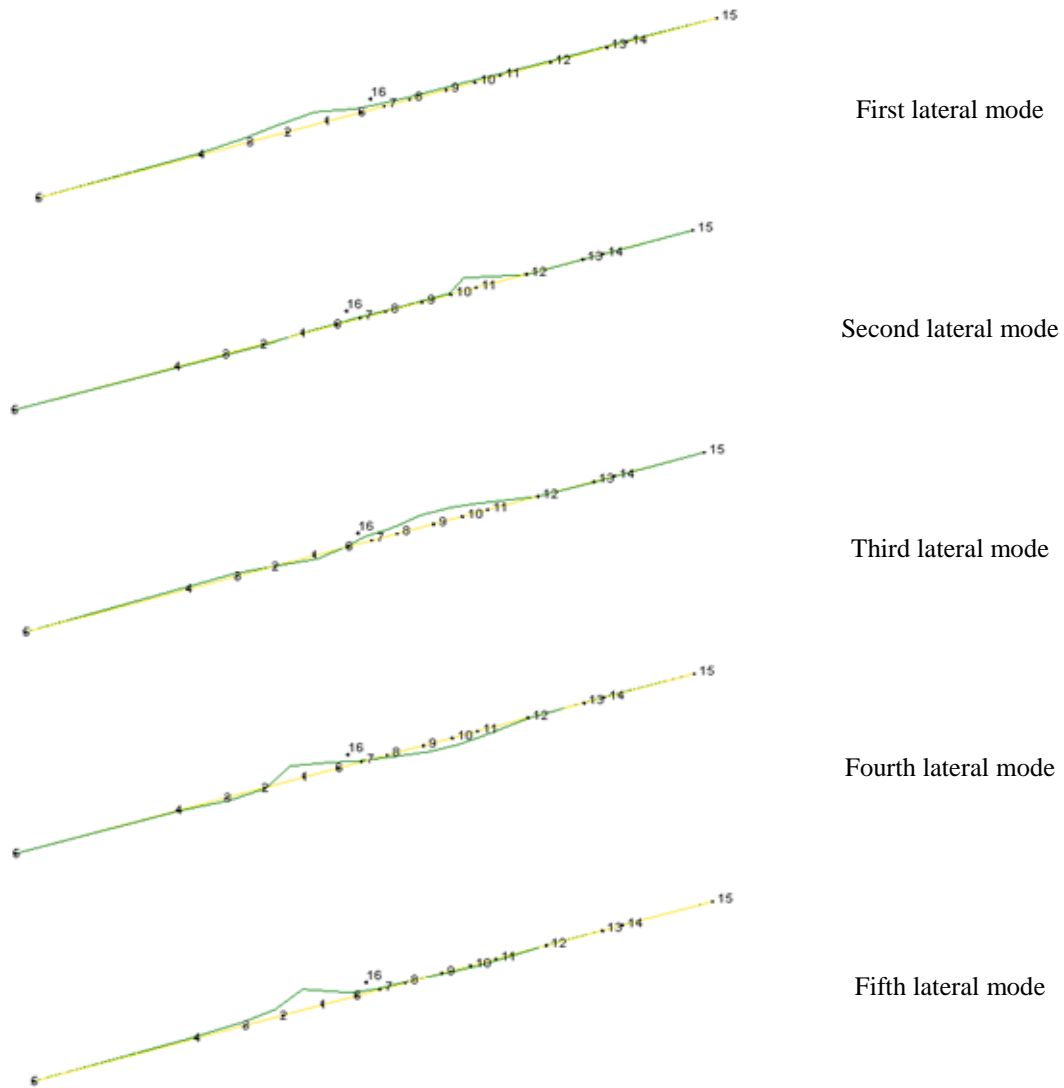


Fig. 14 The first five mode shapes of Aspendos Masonry Arch Bridge

It was observed that there are big differences in the first five natural frequencies. The maximum difference was occurred in the second mode and the average difference was approximately 80%.

To decrease the differences, the initial analytical model was calibrated by considering the damage effects and river bed condition. Manual updating method (trial and error) was used and the in-situ observations were applied to the initial finite element model. Therefore, the coefficient of soil reaction was considered as  $96 \cdot 10^6 \text{N/m}^3$ . The natural frequencies for the calibrated case are given in Table 4 and the mode shapes are presented in Fig. 15. By the calibrating process, the average difference was decreased to considerably. It can be stated that the calibrated finite element model reflects the real behavior of the bridge more accurately than the initial finite element model.

The calibrated model was analyzed by the dead, live, earthquake and overflow. The analyses results were evaluated by using three load combinations derived from these loads. These are given as below:

- First Combination : Dead Load + Live Load
- Second Combination : Dead Load + Live Load + Earthquake Load
- Third Combination : Dead Load + Live Load + Overflow Load

Table 4 The calibrated analytical natural frequencies of Aspendos Bridge

Mode Number	Natural Frequency (Hz)
1	5.68
2	8.08
3	10.67
4	11.17
5	12.64

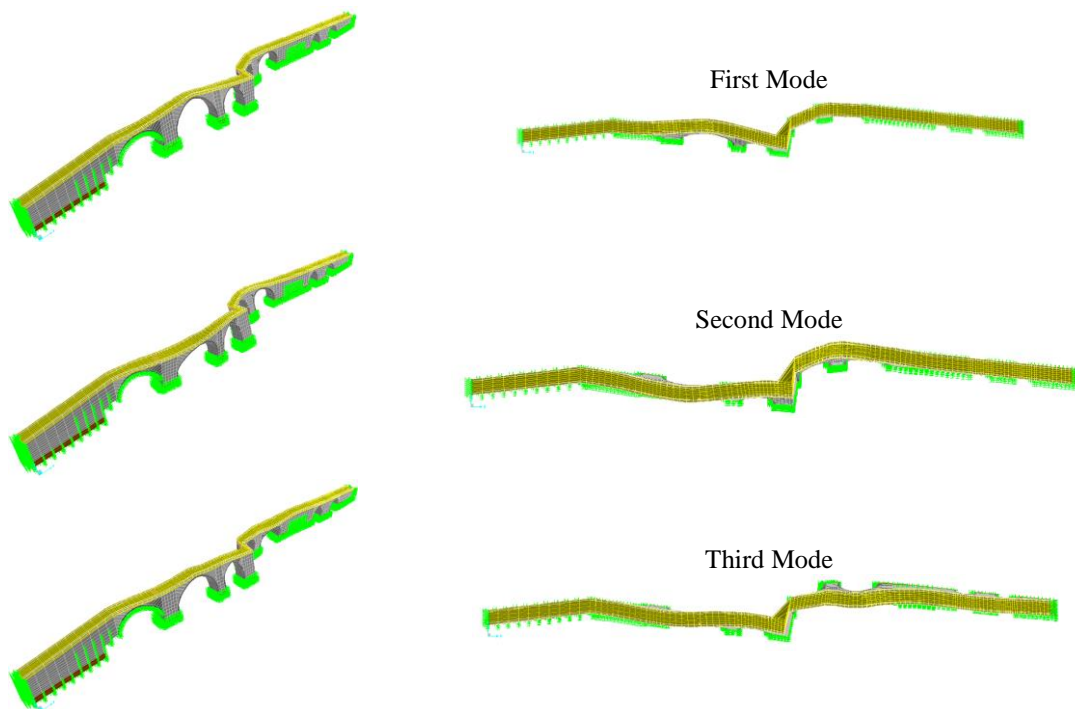


Fig. 15 The first five mode shapes of Aspendos Bridge from the calibrated finite element model

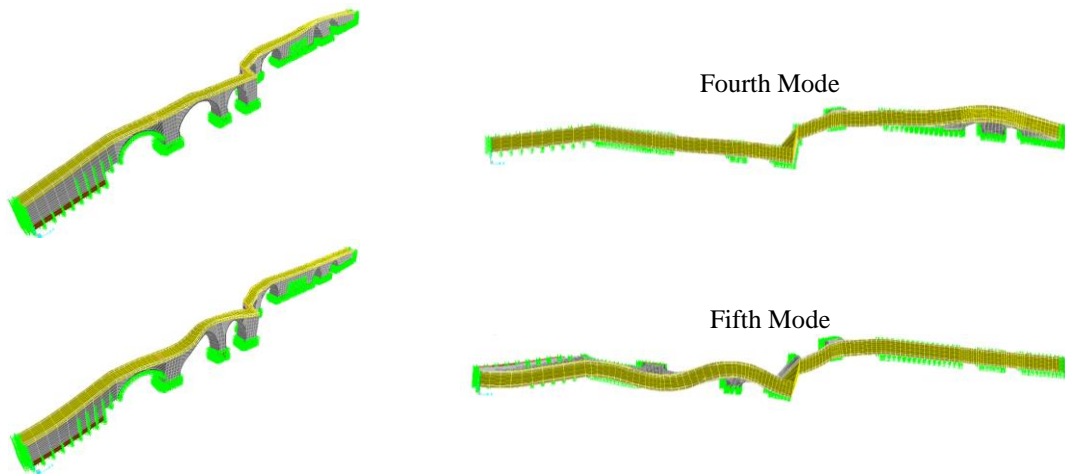


Fig. 15 Continued

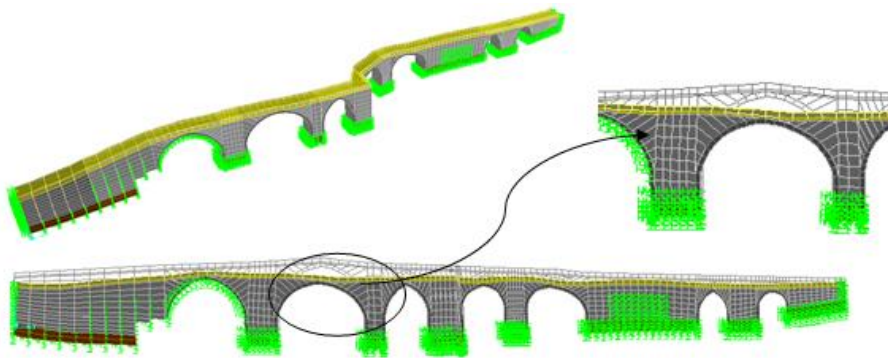


Fig. 16 The displacement of the bridge under the dead load

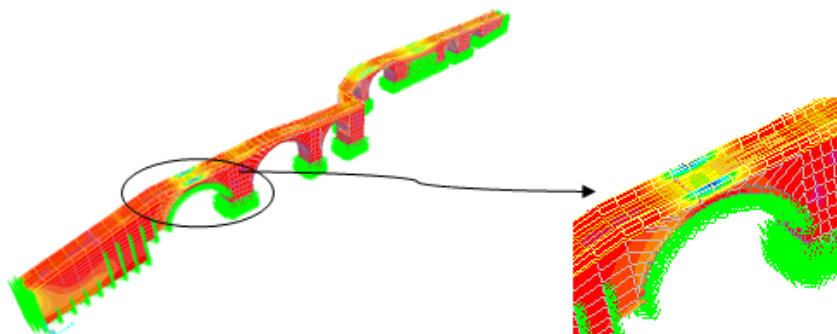


Fig. 17 The distribution of the tensile stress on the bridge under the dead load

#### 4.1 Dead Load Analysis

Firstly, Aspendos Masonry Arch Bridge was analyzed for the dead load. The displacements, tensile stress and compressive stress were attained under this load case as shown in Figs. 16-18.

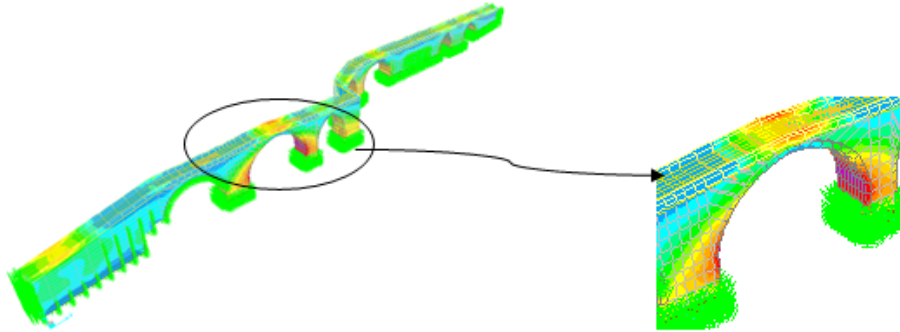


Fig. 18 The distribution of the compressive stress on the bridge under the dead load

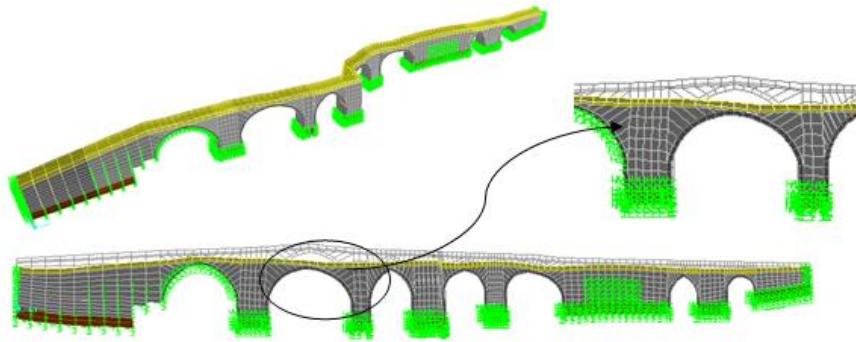


Fig. 19 The displacement of the bridge under the live load

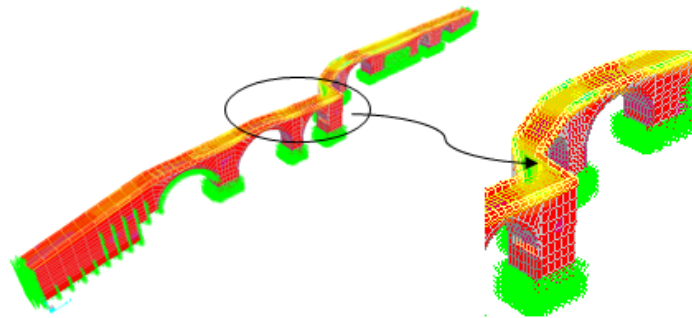


Fig. 20 The distribution of the tensile stress on the bridge under the live load

The maximum displacement occurred in the second span in the vertical direction as 1.08mm. The maximum tensile stress occurred in the first span as 0.36MPa, the maximum compressive stress was occurred in the second span, which is the biggest span, as 0.60Mpa.

#### 4.2 Live load analysis

Secondly, Aspendos Masonry Arch Bridge was analyzed for the live load, which is 500kN/m<sup>2</sup>. The displacements, tensile stress and compressive stress were attained under this load case as shown in Figs. 19-21.

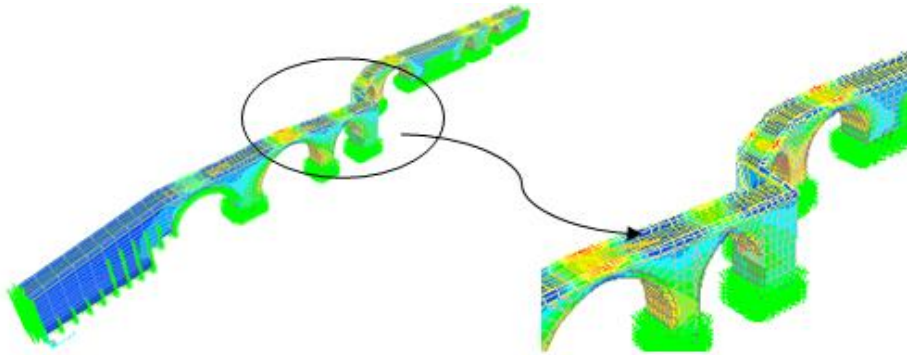


Fig. 21 The distribution of the compressive stress on the bridge under the live load

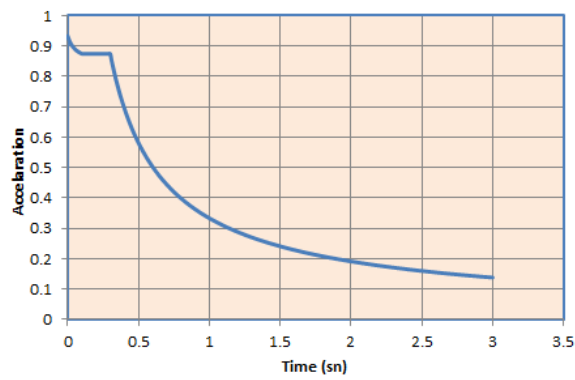


Fig. 22 The response spectrum used in the earthquake analysis

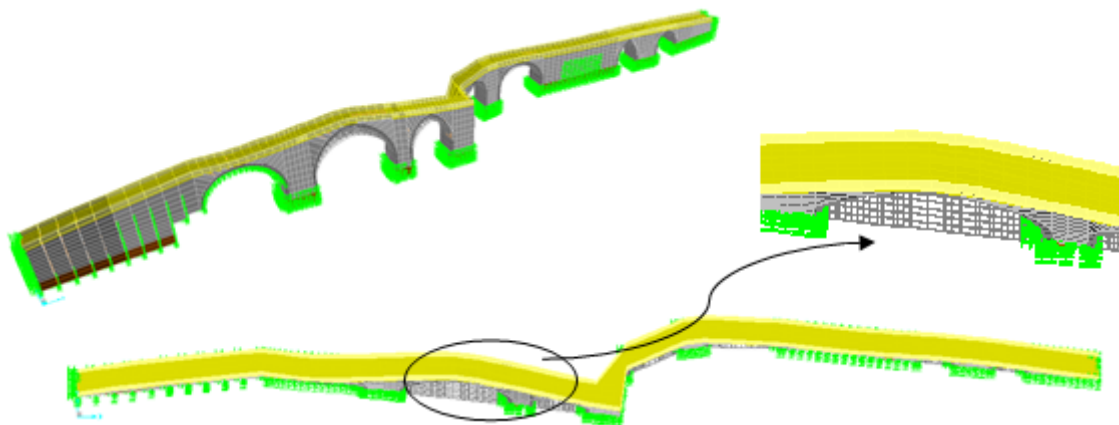


Fig. 23 The displacement of the bridge under the earthquake load

The maximum displacement occurred in the second span in the vertical direction as 0.2mm. The maximum tensile stress occurred in the fifth span as 0.12MPa, the maximum compressive stress was occurred in the second, fifth and sixth spans as 0.18Mpa.

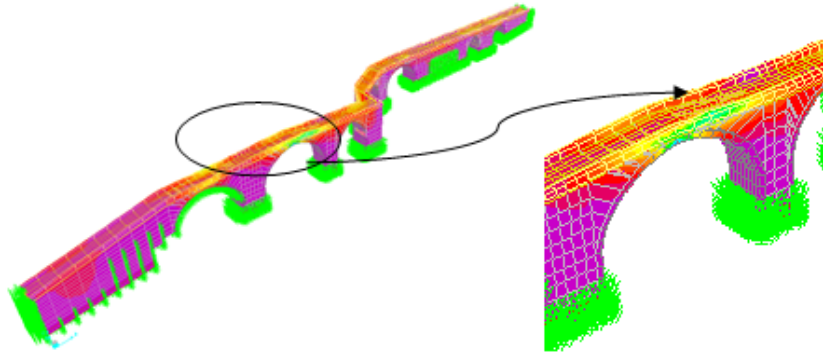


Fig. 24 The distribution of the tensile stress on the bridge under the earthquake load

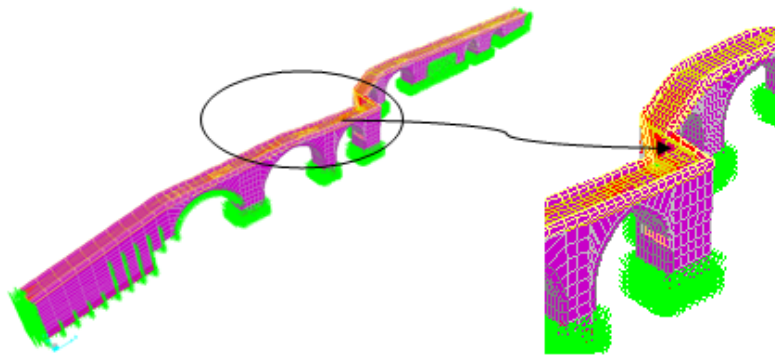


Fig. 25 The distribution of the compressive stress on the bridge under the earthquake load

#### 4.3 Earthquake load analysis

Thirdly, Aspendos Masonry Arch Bridge was analyzed for the earthquake load. Because earthquake motions are random and dependent on factors such as local soil conditions and distance from the source, it is most practical to use response spectra for earthquake loads. Therefore, the earthquake analysis was performed by using response spectrum analysis method, which was defined according to the Turkish Earthquake Guide (DBYYHY 2007). The region is in the second seismic zone depicted in Seismic Zoning Map of Turkey prepared by the Ministry of Public Works and Settlement. The used response spectrum is given in Fig. 22. The displacements, tensile stress and compressive stress were attained under this load case as shown in Figs. 23-25.

The maximum displacement occurred in the second span in the lateral direction as 3.7mm. The maximum tensile stress occurred in the second span as 1.54MPa, the maximum compressive stress was occurred in the fifth span as 0.84Mpa.

#### 4.4 Water load analysis

Finally, Aspendos Masonry Arch Bridge was analyzed for the river water load. The water pressure was calculated according to the maximum water level. The water loads were applied to the upstream face. The displacements, tensile stress and compressive stress were attained under this load case as shown in Figs. 26-28.

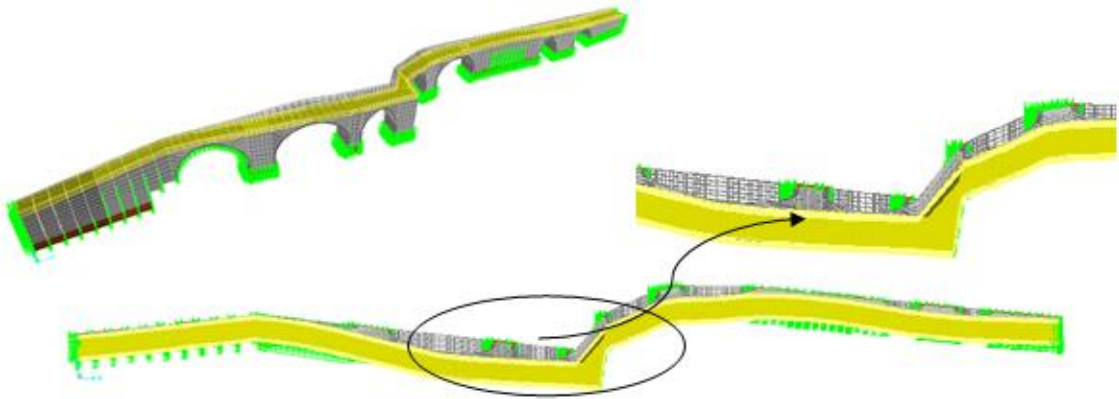


Fig. 26 The displacement of the bridge under the river water load

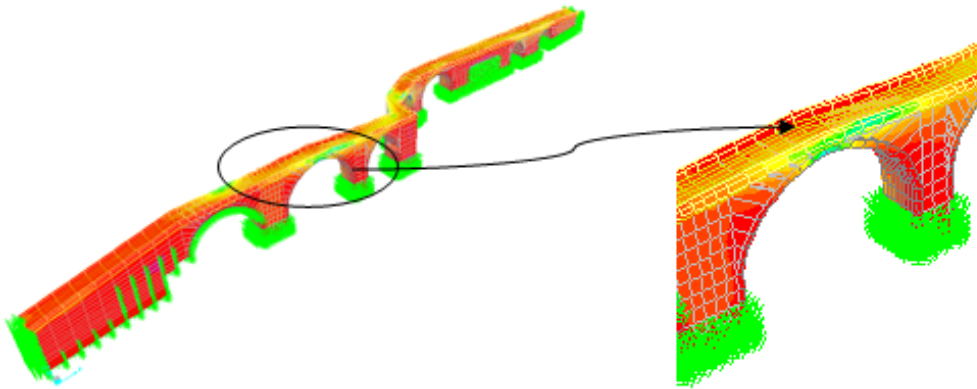


Fig. 27 The distribution of the tensile stress on the bridge under the river water load

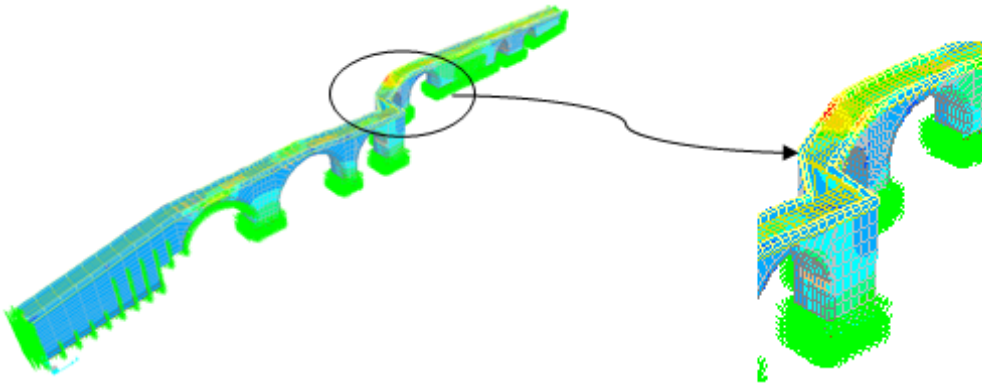


Fig. 28 The distribution of the compressive stress on the bridge under the river water load

The maximum displacement was occurred in the second span in the lateral direction as 7.05mm. The maximum tensile stress was occurred in the second span as 2.28MPa, the maximum compressive stress was occurred in the fifth span as 3.12Mpa.

Table 5 The displacements, compressive and tensile stresses for the loading cases of Aspendos Masonry Arch Bridge

Load Case	Maximum Displacements (mm)	Maximum Tensile Stress (MPa)	Maximum Compressive Stress (MPa)
Dead Load	1.08 (Vertical)	0.36	0.60
Live Load	0.20 (Vertical)	0.12	0.18
Earthquake Load	3.7 (Lateral)	1.54	0.84
Water Load	7.05 (Lateral)	2.28	3.12
First Combination	1.28 (Vertical)	0.42	0.715
Second Combination	3.70 (Lateral) 2.04 (Vertical)	1.50	1.68
Third Combination	6.55 (Lateral) 2.58 (Vertical)	2.40	2.88

## 5. Evaluation of the structural performance of Aspendos Bridge

The structural performance of the bridge was evaluated for the load combinations, which were defined in previous section. Firstly, the displacements, compressive and tensile stresses for the loading cases were attained and given in Table 5. Demand-capacity ratio (DCR) was used to determine the structural performance. The ratio was selected as 1.5 ( $D/C=1.5$ ) depending on the natural frequencies of the structure (Rota, 2004). Therefore, it can be said that the bridge resists the maximum tensile stress of the mortar as 0.615MPa.

It was observed that the maximum compressive stresses for these load combinations were under the compressive strength of the mortar for all cases. Also, the tensile stresses cannot exceed the tensile strength of the mortar for the dead, live loads and first load combination. For the other cases, the tensile stresses were over the tensile strength of the mortar. It means that it was possible to create damages for these cases.

## 6. Conclusions

The Aspendos Masonry Arch Bridge was exposed to the earthquakes in the region and the overloading by the river flow especially in the spring of each year. Also, it was restored many times because it was damaged by overflow in Köprüçay River. Lastly, the bridge was damaged by overflow in 2010. Therefore, the structural performance of was evaluated in this study for different load cases and combinations.

First of all, an initial finite element model was created and it was calibrated to reduce the differences in the experimental and analytical frequencies. In this calibration process, the damage effects and river bed condition were applied to the finite element model. After that, the bridge was analyzed for the dead, live, earthquake and overflow loads. The results of the analysis were evaluated according to the three different load combinations. It was observed from the analysis that the maximum displacements and stresses generally occurred in the second arch span. The maximum lateral and vertical displacements were attained as 6.55mm and 2.58mm, respectively, for the third load combination. The maximum tensile stress was occurred as 2.40MPa for the third load combination while the maximum compressive stress was 3.12MPa for only the overflow

analysis. Also, the maximum compressive stresses for these load combinations were under the compressive strength of the mortar for all cases and the tensile stresses under the tensile strength of the mortar for only the dead, live loads and first load combination. But the tensile stresses exceed the tensile strength of the mortar for the other load cases.

It could be stated that the bridge was under risk and it should be restored. Especially, the scouring on the supports must be hampered and the maximum water level must be decreased by regulating the river bed.

### Acknowledgements

This research was supported by the TUBITAK and Karadeniz Technical University under Research Grant No. 106M038 and 2005.112.001.1, respectively. I also thank Prof. Dr. Alemdar BAYRAKTAR who was administrator of these projects.

### References

- Alberto, C., Se Stefano, A., Invernizzi, S., Ruocci, G., Lacidogna, G., Manuello, A., Ceravolo, R., Degiovanni, L. and Quattrone, A. (2010), "Experimental and numerical analysis of a two-span model Masonry Arch Bridge subjected to pier scour", *Adv. Mater. Res.*, **133-134**, 301-306.
- Bayraktar, A. (2011), *Aspendos (Belkis) Bridge Structural Analysis and Evaluation Report*, Karadeniz Technical University, Trabzon, Turkey. (in Turkish)
- Bayraktar, A., Birinci, F., Altunışık, A.C., Türker, T. and Sevim, B. (2009), "Finite element model updating of Senyuva Historical Arch Bridge using ambient vibration tests", *Baltic J. Road Bridge Eng.*, **4**(4), 177-185.
- Bayraktar, A., Altunışık, A.C., Birinci, F., Sevim, B. and Türker, T. (2010), "Finite element analysis and vibration testing of a two-span Masonry Arch Bridge", *J. Perform. Constr. Facil.*, ASCE, **24**(1), 46-52.
- Brenchich, A. and Sabia, D. (2008), "Experimental identification of a multi-span masonry bridge: the Tanaro Bridge", *Construc. Build. Mater.*, **22**, 2087-2099.
- DBYBHY (2007), *Principles About Building Constructed in Earthquake Zone*, The Ministry of Public Works, Ankara, Turkey. (in Turkish)
- Jacobsen, N.J., Andersen, P. and Brincker, R. (2006), "Using enhanced frequency domain decomposition as a robust technique to harmonic excitation in operational modal analysis", *Proceedings of ISMA2006 International Conference on Noise & Vibration Engineering*, Leuven, Belgium.
- Kessener, P. and Piras, S. (1998), *The Aspendos Aqueduct and the Roman-Seljuk Bridge Across the Eurymedon*, The Aspendos Aqueduct Research Project (AARP)-1995.
- Klaus, G. (1999), *Im Zickzack-Kurs über den Fluß. Die römisch/seldschukische Eurymedon-Brücke von Aspendos (Türkei)*, *Antike Welt*, **30**, 1, 1-12. (in German)
- OMA (2006), *Operational Modal Analysis, Release 4.0*. Structural Vibration Solution A/S, Denmark.
- Peeters, B. (2000), "System identification and damage detection in civil engineering", PhD Thesis, K.U, Leuven, Belgium.
- Pela, L., Aprile, A. and Benedetti, A. (2009), "Seismic assessment of Masonry Arch Bridges", *Eng. Struct.*, **31**(8), 1777-1788.
- Pela, L., Aprile, A. and Benedetti, A. (2012), "Comparison of seismic assessment procedures for Masonry Arch Bridges", *Construct. Build. Mater.*, 1-14.
- PULSE (2006), *Analyzers and Solutions, Release 11.2*, B&K, Sound and Vibration Measurement A/S, Denmark.
- Ramos, L.F., Lourenço, P.B. and Costa, A.C. (2005), "Operational modal analysis for damage detection of a

- Masonry construction”, *Proceedings of the 1<sup>st</sup> International Operational Modal Analysis Conference*, Denmark, April.
- Rota, M. (2004), “Seismic vulnerability of Masonry Arch Bridges walls”, MSc. Thesis, European School of Advanced Studies in Reduction of Seismic Risk (Rose School), Italy.
- Rota, M., Pecker, A., Bolognin, D. and Pinho, R. (2005), “A methodology for seismic vulnerability of Masonry Arch Bridge walls”, *J. Earthq. Eng.*, **9**(2), 331-353.
- SAP2000 (2008), *Integrated Finite Element Analysis and Design of Structures*, Computers and Structures Inc, Berkeley, California, USA.
- URL-1, 19.12.2012. [http://tr.wikipedia.org/wiki/Türkiye'deki\\_tarihi\\_köprüler](http://tr.wikipedia.org/wiki/Türkiye'deki_tarihi_köprüler).
- URL-2, 19.12.2012. [.http://tr.wikipedia.org/wiki/Mostar\\_Köprüsü](http://tr.wikipedia.org/wiki/Mostar_Köprüsü).
- URL-3, 19.12.2012. [http://en.wikipedia.org/wiki/Eurymedon\\_Bridge\\_\(Aspendos\)](http://en.wikipedia.org/wiki/Eurymedon_Bridge_(Aspendos)).